

Computation and Measurement of the Fading Rate of Moon-Reflected UHF Signals¹

S. J. Fricker, R. P. Ingalls, W. C. Mason, M. L. Stone, and D. W. Swift²

(April 29, 1960)

A method is described for predicting the fast fading rate of moon-reflected signals. It is based entirely upon considerations of the observer-moon positions and relative motions. Experimental results which are in good agreement with the computed fading rates have been obtained from a moon-reflection experiment at a frequency of 412 megacycles per second. Some possible implications of this method of interpreting fading rates are given.

1. Introduction

The effect on UHF signals of transmission through the ionosphere and into space is becoming a problem of increasing importance. At present the characteristics of the transmission medium are not known in detail, and the effects upon transmitted signals remain questionable.³ It is known that under certain conditions, e.g., auroral activity, the disturbances are such that radar returns may be obtained from them. While this provides valuable information about the backscatter which may be expected, it does not give a direct measure of the effect upon the transmitted signal. Some information may be obtained by making use of the signals received from radio stars; the scintillation rates of such signals have been observed to increase at times of disturbed ionospheric conditions. However, a more controllable extra-terrestrial signal source has some advantages compared with radio stars. Prior to the advent of artificial satellites, it appeared that use of the moon as a reflector was a reasonable means of obtaining such a signal. Moon-reflected signals have been reported for some years [2],⁴ and the use of moon relay circuits for communications purposes is developing, but most of the measurements reported have not been directly applicable to the problem of ionospheric transmission effects upon UHF signals. The results reported in this paper were obtained in the course of a moon-reflection experiment carried out between South Dartmouth, Mass., and Alpha, Md. [3]. The procedures established in this test formed the basis for a later transmission experiment carried out between College, Alaska, and Westford, Mass. It is hoped to publish a full account of this latter experiment at a later date.

Among the results of the test was the direct correlation between the fading rate of the received signal and the predicted calculations of the total libration rate of the moon. The spectral broadening

of the lunar signal was thus shown to be an effect of the motion of the moon. The major portion of this paper is concerned with an outline of these calculations and a demonstration of their agreement with measured values.

2. System Used in the Experiment

The transmitter and 60-ft diam parabolic antenna were located at the M.I.T. field station at Round Hill, South Dartmouth, Mass. (41.5395° N, 70.9512° W). The receiving site was at Alpha, Md. (39.3224° N, 76.9258° W), about 350 miles from South Dartmouth. The receiving system used a 28-ft diam parabolic antenna with two orthogonal feeds. Two identical receiving systems were used with common local oscillators. With a transmitted power of 40 kW at 412 Mc/s and a final receiver bandwidth of 50 c/s, a signal-to-noise ratio of 25 to 30 db was obtained. Paper tape records were made of the detected signals, and periodic magnetic tape recordings were made of the signals at an intermediate frequency of 2,500 c/s. Observations were made from moonrise to moonset each day from 6 August until 29 August 1957.

3. Paper-Tape Recording for Fading-Rate Measurements

Typical recordings of the detected signals are shown in figures 1, 2, and 3. The frequency of the "fading" shown is a prominent feature, and during

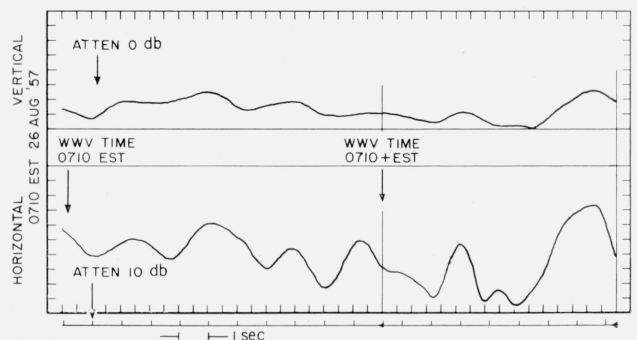


FIGURE 1. Fast recording of detected signal, slow fading rate. (Traced from original recording chart.)

¹ Contribution from Lincoln Laboratory, Massachusetts Institute of Technology, Lexington 73, Mass. The Lincoln Laboratory is operated with support from the U.S. Army, Navy, and Air Force.

² Present address of D. W. Swift: Avco Research and Advanced Development Division, Wilmington, Mass.

³ A summary of the work in this area through 1956 is given in reference [1].

⁴ Figures in brackets indicate the literature references at the end of this paper.

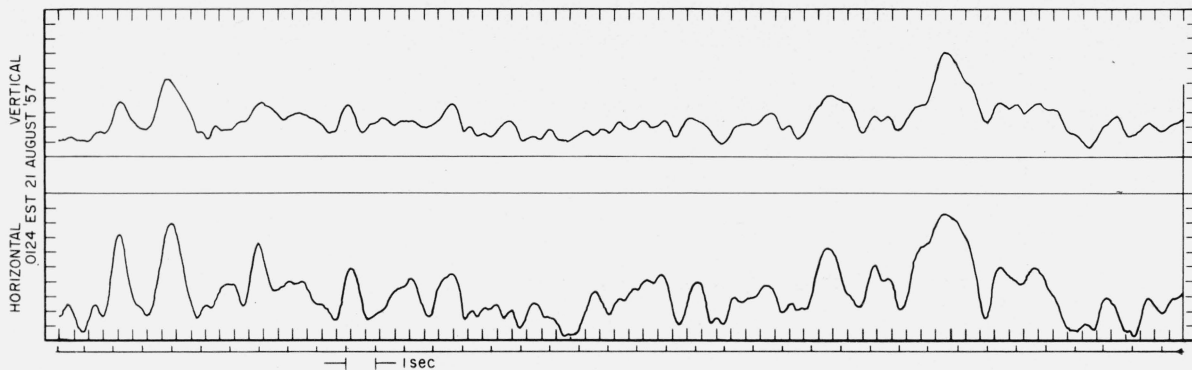


FIGURE 2. Fast recording of detected signal, medium fading rate.
(Traced from original recording chart.)

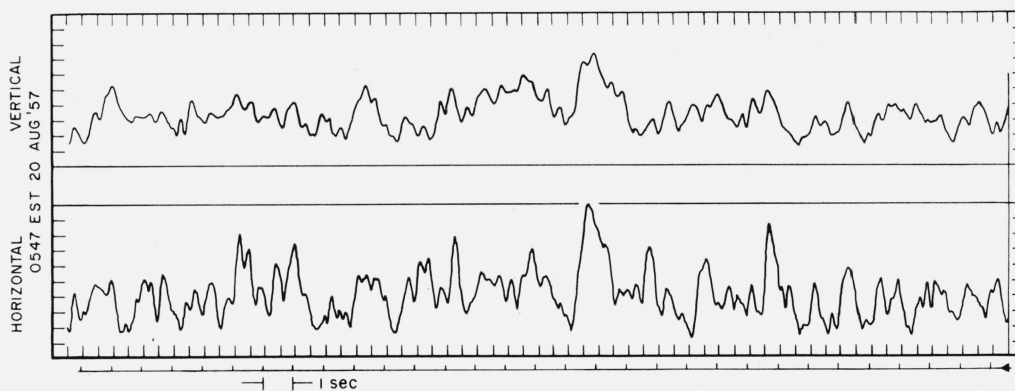


FIGURE 3. Fast recording of detected signal, fast fading rate.
(Traced from original recording chart.)

the test it was found to vary within fairly wide limits. At times the rate appeared to be several cycles per second, at other times the signal level remained almost constant for several minutes. Figure 1 shows a typical section of a recording taken at a relatively slow fading rate period, figure 2 shows an average fading rate, and figure 3 shows one of the faster fading rates. All of these were taken during the test with a detector time constant of 0.15 sec. The magnetic-tape recordings of the 2,500 c/s IF signals formed a convenient stored source of signals to be played back through a detector with an adjustable time constant. Some experimentation was needed to determine a suitable time constant which, it was felt, produced a record that showed up most of the signal variations without being too affected by noise. A value of 0.015 sec for the time constant was chosen as a suitable compromise, and many of the recorded 2,500 c/s IF signals were replayed with this modified detector system. Typical results obtained on a Brush recorder are shown in figures 4 (a) and (b). The paper-tape recordings thus obtained were used to measure the fading rate in a rather arbitrary but consistent manner. This was done simply by counting the number of detected signal maximums occurring over an interval of approximately 1 min at any given period. Results varied from 3 to 4 fades/sec to approximately 0.005 fades/sec. The higher frequencies were observed most of the time, while the very low fading rates

were comparatively infrequent, and lasted for only a short time in any case. Some of the measurements are shown plotted as fading rate versus time of day in figures 11 (a) to (g).

4. Libration-Rate Computations

It seemed to be a reasonable assumption that the effective libration of the moon had a large part to play in producing the varying fading rates of the moon-reflected signals [2]. (The computations to be described first determine what is termed here the "total libration rate" of the moon, and thus proceed to calculate the resulting "Doppler spread." This can then be interpreted as a fading rate, and compared with the measured fading rate.)

An overall view of the geometry involved in the calculation may be useful. Figure 5 shows a simplified sketch of the earth-moon system. In effect, the moon presents a slightly varying face to the earth, due to the dynamics of its motion. This means that an observer on earth looking toward the center of the moon does not always see the same surface point (A in fig. 5), but rather a changing point on the surface. The motion involved is described by the selenographic latitude and longitude figures listed in the *American Ephemeris and Nautical Almanac*. The axes about which these positions are measured are shown in figure 5. In general, the axis for the selenographic latitude variations is inclined to the celestial equator.

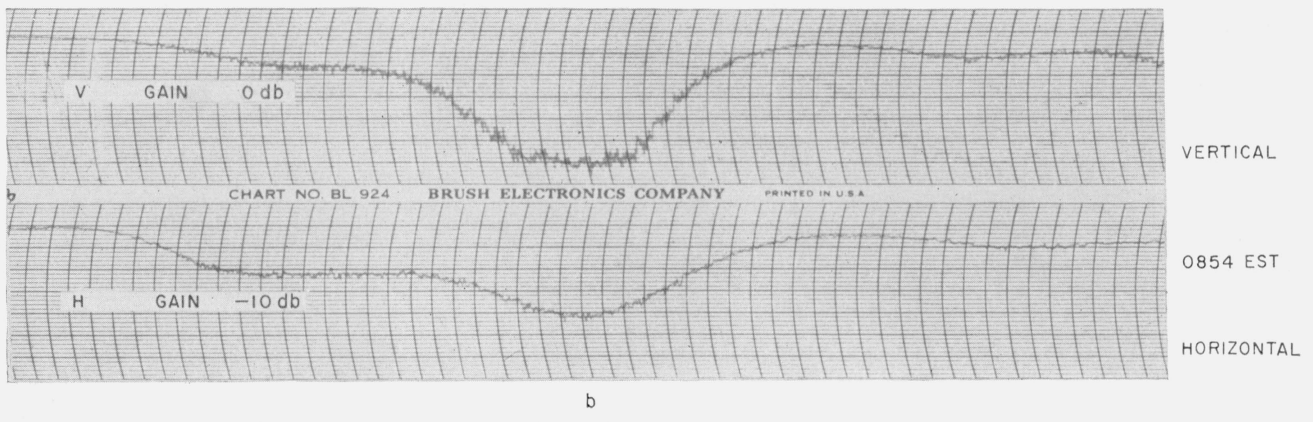
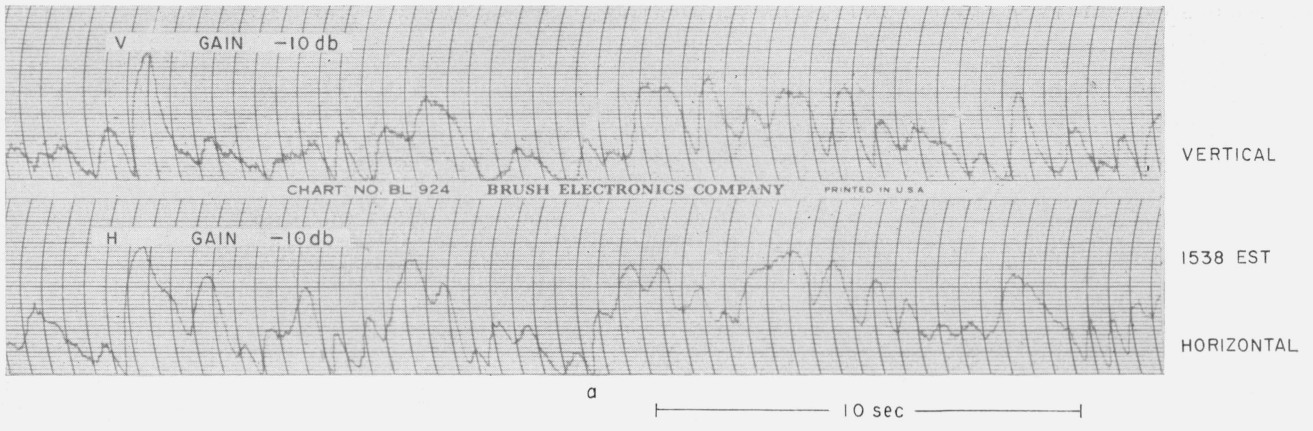


FIGURE 4 a, b. Fast recordings of detected signals with 0.015-sec. time constant.

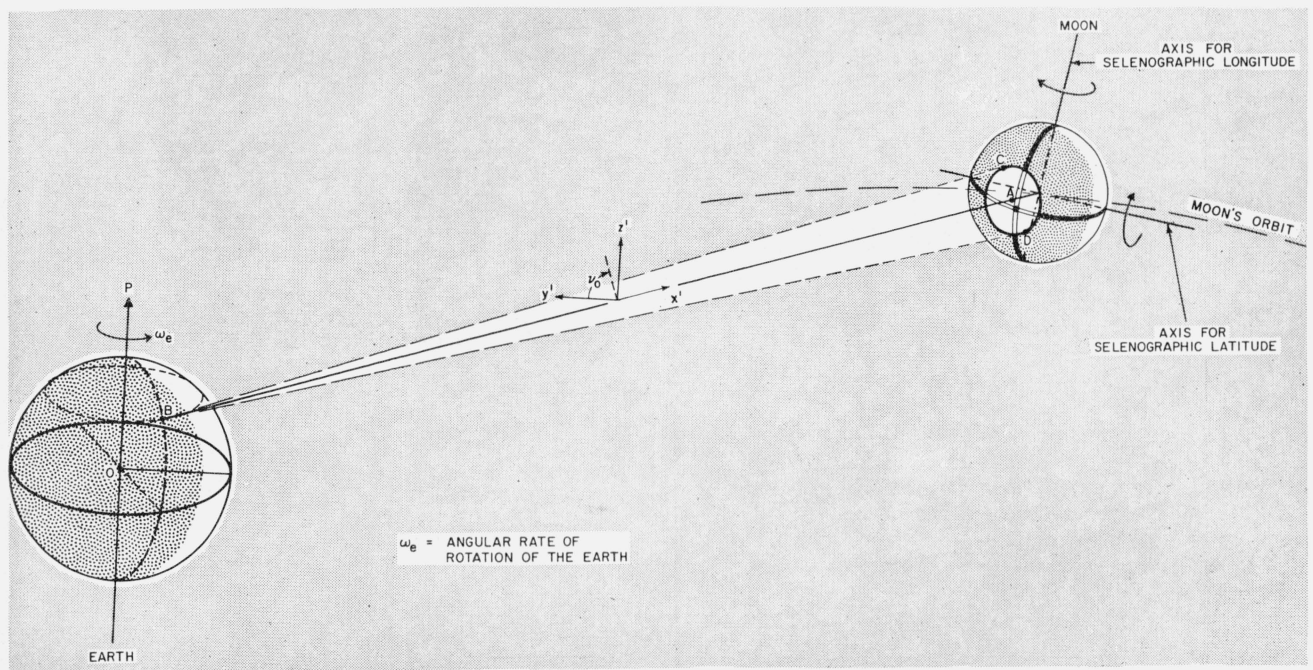


FIGURE 5. Geometry for fading rate computations.

4.1. Moon's Position

An observer on earth, at point B, must look in the direction BA in order to see the moon. Then, due to the earth's rotation about the axis OP, the ray BA sweeps across the moon's surface. On addition, the combination of these two effects give rise to what is termed the "total libration" of the moon. A system of axes can be set up, and the motion of the moon can be resolved along the same set of axes. Combination of the two sets of components is then a simple matter. In effect, expressions are derived for the total libration rates in latitude and longitude, l_{TB} and l_{TL} , respectively, of the form

$$l_{TB} = (l'_B + f_1),$$

and

$$l_{TL} = (l'_L + f_2),$$

where l'_B and l'_L are libration rates due to the moon's motion, and f_1 and f_2 are equivalent functions due to the earth's motion. All the functions, of course, are time-dependent. The total libration rate is given by the square root of the sums of the squares of l_{TB} and l_{TL} . Hence, both of these quantities must become small in order to give a low value for the total effective libration rate.

With the libration rate computed, the next step is to transform it into an effective fading rate. Suppose that instantaneously the moon had only one strongly reflecting region located centrally at point A, so that a cw signal reflected from this region would show only the main Doppler shift in frequency. If now two additional reflecting portions are assumed to exist at C and D, toward the rim of the moon and symmetrically located with respect to the center portion, then each of these regions would be in motion due to the effective libration of the moon. The component of this motion resolved along the direction to the observer would give rise to a small additional "Doppler spread," so that an incident cw signal would be reflected with two Doppler sidebands. Reception and detection of this signal would then show a signal of varying level, with the Doppler spread in effect producing the "fading rate." Now actually a large portion of the moon must be effective in giving rise to appreciable reflections, and each small contributing area gives rise to its own particular Doppler spread. Integration over the whole surface is difficult, since the reflection mechanism is by no means well understood, and the moon is a rough body. However, it is possible to examine the moon's surface to determine the maximum extent of the Doppler spread. Consider a circle drawn on the moon's surface, the radius of this circle being specified as a given fraction of the actual full radius of the moon. All points on this circle can then be examined to determine that point which gives rise to the maximum magnitude of Doppler spread. If the point C on the moon's surface is considered to be the point in question, then its position on the circle is specified by the angle ν_0 , measured from the y' axis. It is apparent that major emphasis in the calculation must be given to a careful consideration of the geometry involved.

Figure 6 shows a sketch of the celestial sphere with the celestial equator in the same plane as the earth's equator. The ecliptic has its ascending node on the celestial equator at the point γ , the vernal equinox, while the ascending node of the moon's orbit on the celestial equator is marked by the point γ' . The moon is assumed to be at the point B, so that the right ascension of the moon, RA_m , is given by the arc γC , and the declination, δ_m , by CB .

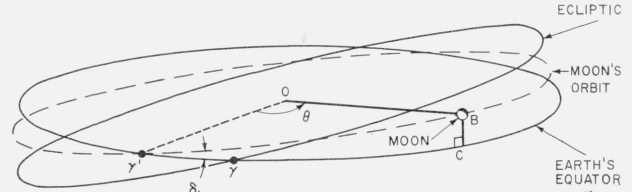


FIGURE 6. Moon-position geometry.

The angle θ is measured in the plane containing the radii $O\gamma'$ and OB , and is taken to be positive in the direction from $O\gamma'$ to OB . The angle δ_i is the inclination angle of the great circle, centered at O , and passing through the points γ' and B .

At any particular time the position of the point γ' is given by noting the value of the moon's right ascension during the preceding month when its declination is zero, and when it is changing from negative to positive values. Hence, with this value of right ascension RA_0 in degrees, $\gamma'\gamma$ is given by

$$\gamma'\gamma = 360^\circ - RA_0,$$

and

$$\gamma'C = \gamma'\gamma + RA_m \quad (2)$$

Thus, from the triangle $\gamma'CB$, the angle θ is specified by

$$\cos\theta = \cos(\gamma'\gamma + RA_m) \cos\delta_m, \quad (3)$$

and

$$\delta_i = 2 \arcsin \sqrt{\frac{\sin(S-\theta) \sin(S-\gamma'\gamma-RA_m)}{\sin\theta \sin(\gamma'\gamma+RA_m)}} \quad (4)$$

where

$$S = [\theta + \gamma'\gamma + RA_m + |\delta_m|]/2.$$

4.2. Orientation of Moon in its Orbit

Figure 7 shows the moon's equatorial plane, with its ascending node on the celestial equator designated as γ'' . The angle Ω' is defined as the distance along the celestial equator from the true equinox to the ascending node of the moon's mean equator, so that the arc $\gamma'\gamma''$ is given by

$$\gamma'\gamma'' = \Omega' + \gamma'\gamma \quad (5)$$

Consider two vectors \bar{A}_1, \bar{A}_2 , where the vector \bar{A}_1 is parallel to the equatorial plane of the moon and perpendicular to OB , while \bar{A}_2 is orthogonal to \bar{A}_1

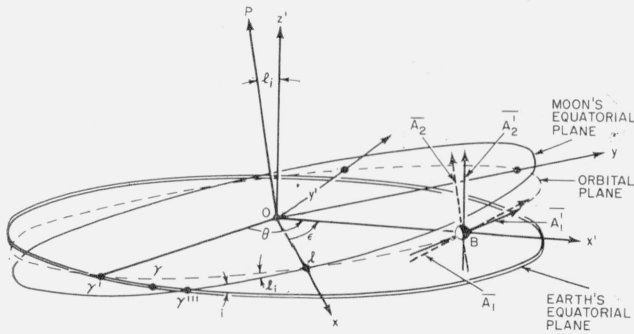


FIGURE 7. Moon orientation geometry.

and normal to the equatorial plane and directed upward. These vectors describe the axes about which the moon's selenographic latitude and longitude are measured. For computational purposes, it is convenient to transform these two vectors into two vectors \bar{A}'_1, \bar{A}'_2 , where \bar{A}'_1 is in the moon's orbital plane, perpendicular to OB , and \bar{A}'_2 is orthogonal to \bar{A}'_1 and OB . Let three unit vectors be defined as follows:

$\bar{i}_{x'}$ = unit vector in direction OB ,

$\bar{i}_{z'}$ = unit vector in direction OZ (OZ perpendicular to orbital plane),

$\bar{i}_{p'}$ = unit vector in direction OP (OP perpendicular to equatorial plane).

Consider an xyz -axis system, with the x -axis coincident with Ol and with the y -axis in the orbital plane. Then the angle ϵ is defined as the angle from the x -axis to OB , measured in the orbital plane. The angle l_i is the included angle $\gamma'l\gamma'''$ (see fig. 7).

Unit vectors $\bar{i}_{a'}$, $\bar{i}_{y'}$, in the direction of \bar{A}'_1 and \bar{A}'_2 respectively, are given by

$$\bar{i}_{a'} = \frac{\bar{i}_p \times \bar{i}_{x'}}{|\bar{i}_p \times \bar{i}_{x'}|} \quad (6)$$

and

$$\bar{i}_{y'} = \bar{i}_{z'} \times \bar{i}_{x'}. \quad (7)$$

The vectors \bar{A}'_1, \bar{A}'_2 can be described with the aid of unit vectors as

$$\bar{A}'_1 = A_1 \bar{i}_{a'} \quad (8)$$

and

$$\bar{A}'_2 = A_2 (-\bar{i}_{y'} \sin l_i + \bar{i}_{z'} \cos l_i). \quad (9)$$

The relations between the two sets of vectors \bar{A}'_1, \bar{A}'_2 and \bar{A}_1, \bar{A}_2 give the following expressions for the magnitudes A'_1 and A'_2 :

$$A'_1 = (\bar{A}_1 + \bar{A}_2) \cdot \bar{i}_{y'} = \frac{A_1}{\sqrt{1 + \cos^2 \epsilon \tan^2 l_i}} - A_2 \sin l_i \cos \epsilon \quad (10)$$

$$A'_2 = (\bar{A}_1 + \bar{A}_2) \cdot \bar{i}_{z'} = \frac{A_1 \cos \epsilon \tan l_i}{\sqrt{1 + \cos^2 \epsilon \tan^2 l_i}} + A_2 \cos l_i \quad (11)$$

The angle i is defined as the inclination of the moon's mean equator to the earth's true equator. With knowledge of $\gamma'\gamma''', i$ and δ_i , the triangle $\gamma'\gamma''l$ can be solved for l_i to give

$$l_i = \arccos [\cos \delta_i \cos i + \sin \delta_i \sin i \cos (\gamma'\gamma''')] \quad (12)$$

and

$$\gamma'l = \arccos \left[\frac{\cos \delta_i \cos l_i - \cos i}{\sin \delta_i \sin l_i} \right]. \quad (13)$$

With the angle θ obtained from (3) and $\gamma'l$ from (13), the angle ϵ is given by

$$\epsilon = \theta - \gamma'l. \quad (14)$$

4.3. Effect of Nonspherical Earth

If a meridional cross section of the earth is assumed to be elliptical in shape, then each point on the surface has a geocentric latitude that is slightly different from its normal geographic latitude. In addition, of course, the radius from the center point of the earth to the observer varies with latitude. The relations among the following parameters:

a_{eq} = equatorial radius of earth,

r = radius to point at geocentric latitude ϕ_c ,

e = ellipticity,

ϕ_c = geocentric latitude,

ϕ = geographic latitude,

are given by

$$r^2 = \frac{a_{eq}^2 (1 - e^2)}{1 - e^2 \cos^2 \phi_c}, \quad (15)$$

$$\tan \phi_c = (1 - e^2) \tan \phi, \quad (16)$$

$$e^2 = 0.006768658.$$

4.4. Doppler Shift of Moon-Reflected Signal

The sketch shown in figure 8 demonstrates the geometry involved. In essence, for an observer at position A , it is necessary to calculate the rate of change of the distance D . The moon's position is given by the distance D_0 and the coordinates shown in figure 9. It is necessary to note the distinction between the two sets of coordinates shown in this figure. The unprimed set is related to the earth's equatorial plane, while the primed system is related to the moon's orbital plane. The following parameters are shown in figures 8 and 9.

D_0 = distance from center of earth to center of moon,

D = distance from observer at A to moon's center,

a_a = distance between earth's center and observer at A ,

ψ = angle between D_0 and a_a ,

δ_i = angle between earth's equatorial plane and the moon's orbital plane,

$\gamma' C$ = right ascension of moon $+ \gamma' \gamma$,

δ_m = declination of moon,

ϕ_a = geocentric latitude of observer,

$\gamma' D$ = right ascension of observer $+ \gamma' \gamma$.

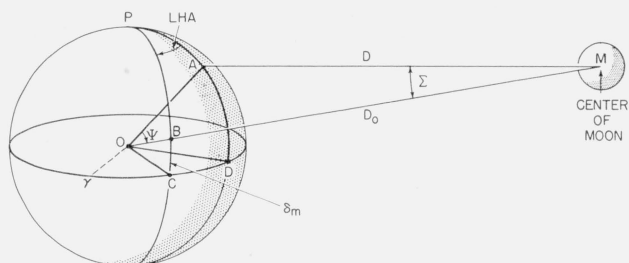


FIGURE 8. Geometry for distance from observer to moon.

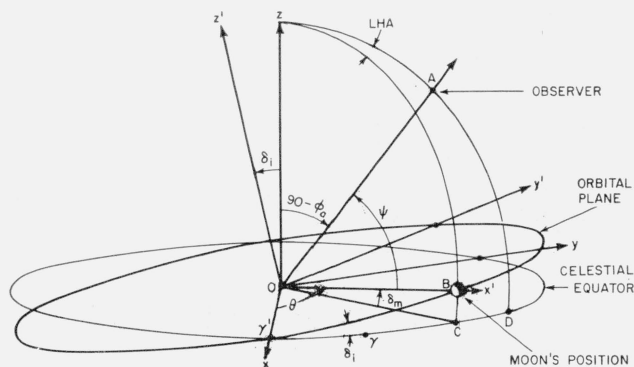


FIGURE 9. Geometry for positions of observer and moon.

In order to express the angle ψ in terms of the position parameters two unit vectors are introduced. A unit vector \bar{i}_a is defined in the direction OA , while \bar{i}_x' is defined as a unit vector in the direction of D_0 in figure 8 (OB in fig. 9). These vectors may be expressed as

$$\bar{i}_a = \bar{i}_z \sin \phi_a + \bar{i}_x \cos \phi_a \cos (\gamma' D) + \bar{i}_y \cos \phi_a \sin (\gamma' D), \quad (17)$$

and

$$\bar{i}_x' = \bar{i}_z \sin \delta_m + \bar{i}_x \cos \delta_m \cos (\gamma' C) + \bar{i}_y \cos \delta_m \sin (\gamma' C) \quad (18)$$

The angle ψ is given by

$$\cos \psi = \bar{i}_x' \cdot \bar{i}_a$$

$$\therefore \cos \psi = \sin \delta_m \sin \phi_a + \cos \phi_a \cos \delta_m \cos (LHA) \quad (19)$$

where LHA is the local hour angle of the moon, and may be expressed as

$$LHA = (\gamma' D) - (\gamma' C) = (\gamma D) - (\gamma C)$$

Now the rate of change of the distance D is given by

$$\begin{aligned} \dot{D} &= \frac{d}{dt} \sqrt{D_0^2 + a_a^2 - 2a_a D_0 \cos \psi} \\ \dot{D} &= \frac{\dot{D}_0(D_0 - a_a \cos \psi) - D_0 a_a \frac{d}{dt} (\cos \psi)}{D} \end{aligned} \quad (20)$$

The values of horizontal parallax, Π , listed in the *American Ephemeris* may be used to compute D_0 , giving

$$D_0 = \frac{a_{eq}}{\sin \Pi}$$

and

$$\dot{D}_0 = -\frac{a_{eq} \cos \Pi}{\sin^2 \Pi} \frac{d\Pi}{dt}$$

It is also necessary to differentiate $\cos \psi$ from eq (19), which in turn involves the rate of change of the local hour angle. In this manner the angular rotation rate of the earth and the rate of change of right ascension of the moon are brought into the computations. Thus

$$\begin{aligned} \frac{d}{dt} (\cos \psi) &= \delta_m [\cos \delta_m \sin \phi_a - \sin \delta_m \cos \phi_a \cos (LHA)] \\ &\quad - \cos \phi_a \cos \delta_m \sin (LHA) \frac{d}{dt} (LHA) \end{aligned}$$

and

$$\frac{d}{dt} (LHA) = \omega_e - \frac{d}{dt} (RA_m),$$

where ω_e is the angular velocity of the earth, and $d/dt (RA_m)$ is the major component of the angular velocity of the moon about the earth.

The above expressions enable \dot{D}_a and \dot{D}_b to be derived for the transmitting and receiving stations, so that the total Doppler shift f_d is given by

$$f_d = -\frac{f_c}{c} (\dot{D}_a + \dot{D}_b) \quad (21)$$

where D_a and D_b now represent the distances between the transmitter and the moon and the receiver and the moon, respectively.

4.5. Libration-Rate Computation

The essence of this computation lies in the description of the motion of a point on the moon's surface as seen by an observer on earth. Part of this motion is due to the actual libration of the moon, and part is due to the movement of the observer. Thus the computations involve the rates of change of the selenographic latitude and longitude, plus the rate of change of some quantity which describes the geometrical earth-moon relationship. The effects of these two physically distinct processes, when added appropriately, then give the total libration rate. It is convenient to use the sign convention used in the *American Ephemeris*. Thus, the selenographic longitudes are measured in the plane of the moon's equator, positive toward the west, the axis of reference being the radius of the moon which passes through the mean center of the visible disk. Latitudes are measured from the moon's equator, positive toward the north.

In section 4.2, two vectors \bar{A}_1, \bar{A}_2 were considered. Now, let \bar{A}_1 become the axial vector \bar{S}_β and \bar{A}_2 become the axial vector \bar{S}_L , where \bar{S}_β and \bar{S}_L represent axes about which the selenographic latitudes and longitudes are measured. The time derivatives of the scalar values of these quantities are given by

$$l_\beta = \frac{dS_\beta}{dt},$$

and

$$l_L = \frac{dS_L}{dt}.$$

Also, in sections 4.2 and 4.4 primed quantities were used with reference to the moon's orbital plane. The same significance again is attached to primed quantities here. Equations (10) and (11) can be rewritten to give S'_β and S'_L , and the resulting expressions differentiated to give

$$\begin{aligned} \frac{dS'_\beta}{dt} = l'_\beta = & \frac{l_\beta}{\sqrt{1 + \cos^2 \epsilon \tan^2 l_i}} - l_L \sin l_i \cos \epsilon \\ & - \left[\frac{S_\beta \cos^2 \epsilon \tan^2 l_i \sec^2 l_i}{(1 + \cos^2 \epsilon \tan^2 l_i)^{3/2}} + S_L \cos \epsilon \cos l_i \right] \frac{dl_i}{dt} \\ & + \left[\frac{S_\beta \cos \epsilon \tan^2 l_i \sin \epsilon}{(1 + \cos^2 \epsilon \tan^2 l_i)^{3/2}} + S_L \sin \epsilon \sin l_i \right] \frac{d\epsilon}{dt}, \end{aligned} \quad (22)$$

and

$$\begin{aligned} \frac{dS'_L}{dt} = l'_L = & \frac{l_\beta \cos \epsilon \tan l_i}{\sqrt{1 + \cos^2 \epsilon \tan^2 l_i}} + l_L \cos l_i \\ & + \left[\frac{S_\beta \cos \epsilon \sec^2 l_i}{(1 + \cos^2 \epsilon \tan^2 l_i)^{3/2}} - S_L \sin l_i \right] \frac{dl_i}{dt} \\ & - \left[\frac{S_\beta \sin \epsilon \tan l_i}{(1 + \cos^2 \epsilon \tan^2 l_i)^{3/2}} \right] \frac{d\epsilon}{dt}. \end{aligned} \quad (23)$$

The effect of the observer's motion may be introduced through use of the parallax angle $\bar{\Sigma}$, shown in figure 8. Consider $\bar{\Sigma}$ to be an axial vector representing a small rotation when the magnitude of $\bar{\Sigma}$ represents the angle between D and D_0 . Hence for small $\bar{\Sigma}$, $\bar{\Sigma}$ is given by

$$\bar{\Sigma} = (\bar{i}_{x'} \cdot \bar{i}_a) \frac{a_a}{D_1} \quad (24)$$

where

$$D_1 = D_0 - a_a \cos \psi \quad (25)$$

In general, the observer's motion will give contributions to both the longitudinal and the latitudinal libration rates. Bearing in mind the association of the primed coordinates with the moon's orbit, and the fact that the selenographic latitudes and longitudes were adjusted to this set of coordinates, it is apparent that the projections of $\bar{\Sigma}$ on the y' and z' axes are required. The component in the z' direction is given by

$$\Sigma_L = (\bar{i}_{x'} \times \bar{i}_a) \cdot \bar{i}_{z'} \frac{a_a}{D_1} = \frac{a_a}{D_1} \bar{i}_a \cdot \bar{i}_{y'} \quad (26)$$

and in the y' direction by

$$\Sigma_\beta = (\bar{i}_{x'} \times \bar{i}_a) \cdot \bar{i}_{y'} \frac{a_a}{D_1} = -\frac{a_a}{D_1} \bar{i}_a \cdot \bar{i}_{z'}. \quad (27)$$

From figure 9, it is seen that

$$\bar{i}_{z'} = \bar{i}_z \cos \delta_i - \bar{i}_y \sin \delta_i \quad (28)$$

and the unit vector $\bar{i}_{y'}$ is given by

$$\bar{i}_{y'} = \bar{i}_{z'} \times \bar{i}_{x'}$$

with $\bar{i}_{z'}$ and $\bar{i}_{x'}$ described by eqs (28) and (18) respectively. The dot products in eqs (26) and (27) may now be expanded to give the components of $\bar{\Sigma}$ as,

$$\begin{aligned} \Sigma_L = \frac{a_a}{D_1} \{ & \cos \delta_i \cos \delta_m \cos \phi_a \sin (LHA) \\ & - \sin \delta_i [\sin \delta_m \cos \phi_a \cos \gamma' D - \cos \delta_m \cos (\gamma' C) \sin \phi_a] \} \end{aligned} \quad (29)$$

and

$$\Sigma_\beta = \frac{a_a}{D_1} [\sin \delta_i \cos \phi_a \sin (\gamma' D) - \cos \delta_i \sin \phi_a] \quad (30)$$

The above two equations can be differentiated to give their rates of change. This involves a number of terms, as most of the parameters are time dependent. However $\gamma' \gamma$ and δ_i change so slowly that negligible error is introduced by assuming them to be constant. The terms thus involve the rate of change of the distance, \dot{D}_1 ; the angular rotation rate of the earth ω_e ; and the rates of change of the moon's right ascension and declination. Hence $\dot{\Sigma}_L$ and $\dot{\Sigma}_\beta$

may be expressed as

$$\begin{aligned} \dot{\Sigma}_L = & -\frac{\dot{D}_1}{D_1} \Sigma_L + \omega_e \frac{a_a}{D_1} \cos \varphi_a [\cos \delta_i \cos \delta_m \cos (LHA) + \sin \delta_i \sin \delta_m \sin (\gamma'D)] \\ & - \frac{d}{dt} (RA_m) \cos \delta_m \frac{a_a}{D_1} [\cos \delta_i \cos \varphi_a \cos (LHA) + \sin \delta_i \sin \varphi_a \sin (\gamma'C)] \\ & - \frac{a_a}{D_1} \dot{\delta}_m \{ \sin \delta_m \cos \delta_i \cos \varphi_a \sin (LHA) \\ & + \sin \delta_i [\cos \delta_m \cos \varphi_a \cos (\gamma'D) + \sin \delta_m \cos (\gamma'C) \sin \varphi_a] \} \end{aligned} \quad (31)$$

and

$$\dot{\Sigma}_\beta = -\frac{\dot{D}_1}{D_1} \Sigma_\beta + \omega_e \frac{a_a}{D_1} \sin \delta_i \cos \varphi_a \cos (\gamma'D), \quad (32)$$

where

$$\dot{D}_1 = \dot{D}_0 - a_a \frac{d}{dt} (\cos \psi).$$

In obtaining the sum of the effects of the moon's motion and the earth's motion, it must be remembered that a rotation in one sense on earth appears as the opposite sense on the moon. That is, an increase of the parallax angle toward the west or north appears as a rotation of the moon toward the east or south. Hence, the components of the total libration rate for a two-station system are

$$l_{T\beta} = \left\{ l'_\beta - \frac{1}{2} \dot{\Sigma}_{\beta a} - \frac{1}{2} \dot{\Sigma}_{\beta b} \right\} \quad (33)$$

$$l_{TL} = \left\{ l'_L - \frac{1}{2} \dot{\Sigma}_{La} - \frac{1}{2} \dot{\Sigma}_{Lb} \right\} \quad (34)$$

where the subscripts a and b refer to the transmitting and receiving stations. The total libration rate, l_T , is thus given by

$$l_T = \sqrt{l_{T\beta}^2 + l_{TL}^2}. \quad (35)$$

4.6. Doppler Spread of Moon-Reflected Signal

So far, when considering the geometry of the earth-moon system, the reference point on the moon has been its center. The corresponding point seen on the surface of the moon may be imagined to be the main reflecting point. However, as mentioned previously, many other points on the moon's surface are effective as reflectors. Any one such point will be in motion due to the libration of the moon, and in consequence of the fact that its line-of-sight velocity is different from that of the central point, its Doppler frequency will be slightly shifted with respect to that of the central point, i.e., with respect to the main computed Doppler frequency. This shift in Doppler frequency is referred to as the "Doppler spread." Obviously, this will depend upon the position of the offset region as well as on the angular velocities involved. Consequently, in order to obtain an idea of the maximum Doppler spread that may occur over

a given portion of the moon's surface, it is convenient to specify a ring whose radius is a given fraction of the radius of the moon, and to examine this ring from 0° to 360° in order to pick out the maximum value of the Doppler spread.

This method of computing the Doppler spread allows a number of approximations to be made. The choice of which approximations to make can be based upon the magnitude of the total libration rate. When this is not too small, the Doppler spread is of the order of cycles per second, and any refinement in the computation would have a relatively small effect. As the libration rate decreases, so does the magnitude of the Doppler spread, and at some point the errors introduced by the approximate computations may become significant. The overall accuracy depends, of course, upon the accuracy of the input information and, if this is not very precise, any small differences carried in the computations may not show up.

Figure 10 shows a sketch of the geometry involved. The moon's center is at O and the observer at O' . Although only one observer's position is shown, the computations are carried out for two separated stations, i.e., transmitter at station a and receiver at station b . The axes shown at the moon's position refer to the moon's orbit, as mentioned previously, and the quantities l_{TL} and $l_{T\beta}$ are used to describe the moon's apparent rotation about these axes. The circle to be examined is shown as $GLCH$ with radius FL , or kR_m , where R_m is the moon's radius and k is the fractional moon's radius. The position of the point L is specified by giving the value of k and the angle ν , where ν is measured positively upwards from a line parallel to the axis of $l_{T\beta}$.

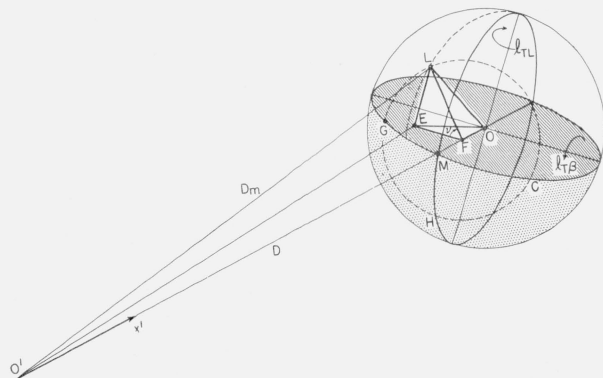


FIGURE 10. Geometry for Doppler-spread computations.

Due to the apparent rotation of the moon about the $l_{T\beta}$ axis, the point L has a component of velocity directed towards $0'$. The approximation is made that station a may be assumed to be at $0'$, so that an observer sees the incremental velocity of point L as

$$v_{a\beta} = kR_m \sin \nu (l'_{\beta} - \dot{\Sigma}_{\beta a}).$$

Rotation about the l_{TL} axis gives a similar component

$$v_{aL} = -kR_m \cos \nu (l'_{L} - \dot{\Sigma}_{La}).$$

The Doppler spread for each station is due to these incremental velocities. The Doppler spread of the transmitted signal plus the Doppler spread of the reflected signal is the total observed Doppler spread. Thus, the Doppler spread due to the moon's libration is

$$\Delta f'_d = f_c \frac{kR_m}{c} [\sin \nu (2l'_{\beta} - \dot{\Sigma}_{\beta a} - \dot{\Sigma}_{\beta b}) - \cos \nu (2l'_{L} - \dot{\Sigma}_{La} - \dot{\Sigma}_{Lb})].$$

Hence with the use of eqs (33) and (34) this may be expressed as

$$\Delta f'_d = 2f_c \frac{kR_m}{c} (\sin \nu \cdot l_{T\beta} - \cos \nu \cdot l_{TL}). \quad (36)$$

There is a small additional Doppler spread term which arises from the fact that the observer is approaching the general point L on the moon's surface, rather than its center. The original main Doppler shift, given by eq (21), was developed for the center point of the moon. Actually it is the rate of change of D_m in figure 10 which should be considered, i.e., $\dot{D}_m = \dot{D} +$ small correction, and this correction will be different for the transmitting and receiving stations. Now $\dot{D}_m \simeq \dot{D}$ may be expressed as $\dot{D}_m = \dot{D} \sqrt{1 - (k^2 R_m^2 / D_m^2)}$. The first term expansion of \dot{D}_m is sufficiently accurate for our purposes, so that with D substituted for D_m in the expansion term the correction is given by

$$\dot{D}_m \simeq \dot{D} - \frac{1}{2} \dot{D} \frac{k^2 R_m^2}{D^2}.$$

Thus the additional Doppler spread term is

$$\Delta f''_d = \frac{1}{2} \frac{f_c}{c} k^2 R_m^2 \left[\frac{\dot{D}_a}{D_a^2} + \frac{\dot{D}_b}{D_b^2} \right] \quad (37)$$

where the subscripts a and b refer to the two stations. The total Doppler spread is now given by

$$\Delta f_d = 2f_c \frac{kR_m}{c} [\sin \nu \cdot l_{T\beta} - \cos \nu \cdot l_{TL}] + \frac{1}{2} \frac{f_c}{c} k^2 R_m^2 \left[\frac{\dot{D}_a}{D_a^2} + \frac{\dot{D}_b}{D_b^2} \right]. \quad (38)$$

The maximum (or minimum) value of the Doppler

spread occurs at the angle ν_0 given by

$$\nu_0 = \arctan [-(l_{T\beta}/l_{TL})]. \quad (39)$$

In order to obtain the maximum Doppler spread value, the positive value of (36) is chosen and added to the absolute magnitude of (37).

When the libration rates are not too small in magnitude (for example, not less than 10^{-7} rad/sec) a number of approximations can be made in the computations. In eqs (31) and (32), terms involving δ_m and $D_1/D_1 \Sigma_{\beta, L}$ can be ignored. The term $\Delta f'_d$ (eq (37)) also may be neglected. Check calculations show that in general a negligible effect is produced by these approximations. For small libration rates their effect needs to be included.

However, it is to be noted that the calculations for the Doppler spread involve the daily values of selenographic latitude and longitude. *The American Ephemeris and Nautical Almanac* lists these to only three significant figures, so that at some point it is to be expected that lack of accuracy in these data will affect the computations. This appears to be the case at periods of very low libration rate.

4.7. Relationship of "Fading Rate" and "Maximum Doppler Spread"

The "fading rate" of the detected signal was determined as outlined in section 3, i.e., by counting the number of maximums in a given time interval. This obviously gives some measure of the form of the returned signal spectrum. It is apparent, physically, that the total signal is due to reflections taking place over much of the moon's surface, probably with a larger weighting factor attached to the central regions. If the spectrum is regarded as similar to that obtained when Gaussian noise is passed through a narrow Gaussian bandpass filter, then work by Rice [4] indicates that the expected number of maximums per second is

$$N \simeq 2.52 \sigma$$

where σ is the standard deviation of the Gaussian filter. Suppose the noise bandwidth, B c/s, is defined as that bandwidth containing half the total power passed by the filter, then

$$B \simeq 1.35 \sigma$$

or

$$B \simeq 0.54 N \text{ c/s.}$$

This gives a relationship between the bandwidth and fading rate that may be useful as applied to the lunar signal. The maximum Doppler spread $(\Delta f_d)_{max}$ is a measure of the change in Doppler experienced at the limb of the moon due to libration. The maximum band limits of the signal, if its spreading were entirely due to libration effects, would be $2\Delta f_d$ corresponding to the range of signal returns from opposite limbs of the moon.

The fading rate of the lunar signal was found to be proportional to the libration rate and hence to the value of $(\Delta f_d)_{max}$. The best fit to the data was found to be given with $k=0.67$ by the empirical formula

$$N = k (\Delta f_d)_{max} = 0.67 (\Delta f_d)_{max}. \quad (40)$$

If our assumed relationship between fading rate and bandwidth is correct, then

$$B = 0.54 \times k (\Delta f_d)_{max} = 0.36 (\Delta f_d)_{max}. \quad (41)$$

The bandwidth obtained is $0.36/2=0.18$ of the maximum possible band limits due to the libration spreading. Since the change in Doppler Δf_d is proportional to the distance from the center of the moon's disk, then it is apparent that most of the signal energy is reflected from a portion of the moon about the center of the face with a fractional radius of only about 0.2.

4.8. Actual Computations

As results were required at intervals of a few minutes over a period of months, the computations were programmed for the IBM 704 and 709 Electronic Data-Processing Machines. Much of the astronomical input data for the program was obtained on standard IBM cards from the U.S. Naval Observatory. Other input quantities were prepared from the American Ephemeris. The machines also were used for additional computations concerned with the antenna orientations.

5. Results Obtained

Figures 11 (a) to (g) show plots of some of the measured fading rates. The computed curves are based on a value of 0.67 in the empirical relationship of (40). The agreement in general is excellent, except at periods of very low fading rate of the order of 0.05 to 0.005 c/s.

In general, the computed values for August 1957 did not fall below approximately 0.1 c/s for either the approximate or the more accurate methods of computation. The approximations involved in the method of computation are capable of allowing a better resolution than this, and it appears that the limiting factor probably is due to the 3-figure accuracy of the published daily values of selenographic latitude and longitude given in the *American Ephemeris and Nautical Almanac*.

The value of k used, 0.67, when inserted in eq (41) for the "noise bandwidth" B , gives

$$B = 0.36 (\Delta f_d)_{max} \text{ c/s.}$$

On this basis the major portion of the reflected signal is obtained from a central disk on the moon, the fractional radius of this disk being approximately 0.2. A different approach is afforded by the results of experiments carried out at the Naval Research

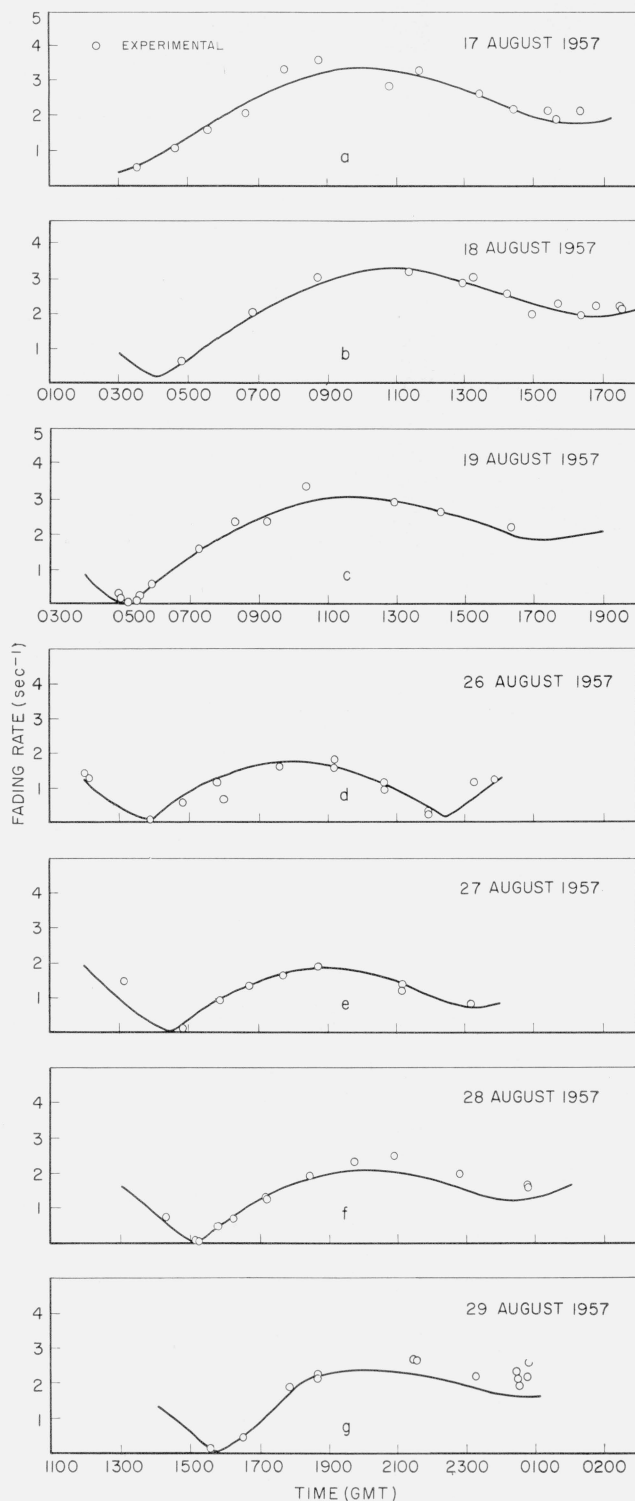


FIGURE 11 a, b, c, d, e, f, g. Comparison of measured and computed fading rates.

Laboratory [5, 6], in which the interpretation of the form of reflected pulsed signals was that only a relatively small central portion of the moon's surface was effective as a reflector.

Although not described here, it is of interest to note that the measured total signal levels showed no evidence of any slow fades. The Faraday rotation was observed, but the total received signal level, after correction for the varying earth-moon distance, was essentially constant.

6. Conclusions

Calculation of the rapid fading rate of moon-reflected signals, in the manner described, has been shown to give results which agree very well with measured values. It appears as if most of the reflected signal may be obtained from a central disk on the moon with a fractional radius of approximately 0.2.

The variation of the position of the region on the moon's surface which gives the maximum Doppler spread is of interest. Table 1 lists values of the angle ν_0 for a typical day, together with the angles of elevation and azimuth. The angle ν_0 depends upon the rates of change of the moon's selenographic latitude and longitude, so that the figures given in table 1 vary from day to day. However, the variation is typical; values of approximately 200° to 300° during moonrise, an increase to values of 10° to 30° while going through transit, and then a further increase to 70° to 130° during moonset. It is apparent that whatever the value of the fractional radius of the moon is taken to be, a considerable portion of the moon's surface is covered during the course of a day. Since the agreement between the computed and measured fading rates is so striking, it would seem that, in its behavior as a reflector or scatterer at 400 Mc/s, the moon's surface is reasonably uniform over quite a large region.

TABLE 1. Variation of angle ν_0 with time for 21 August 1957

Time (21 August 1957) (G.m.t.)	Angle of maximum Doppler spread ν_0 degrees	Moon direction at South Dartmouth	
		Elevation degrees	Azimuth degrees
0600	196	3.9	67.8
0700	229	14.4	76.8
0800	316	25.0	85.9
0900	349	35.9	95.7
1000	359	46.7	107.3
1100	005	56.6	123.0
1200	010	64.5	146.1
1300	016	67.6	179.5
1400	021	64.5	213.1
1500	029	56.5	236.4
1600	038	46.6	252.2
1700	053	36.0	263.5
1800	074	25.0	273.4
1900	102	14.2	282.4
2000	128	3.8	291.3

From the measured signal levels and a knowledge of the parameters of the system, the usual radar equation was applied to give an estimate of the

cross section of the moon. This was

$$\sigma = 7 \times 10^{11} \text{ m}^2.$$

The projected area of the moon is approximately $0.95 \times 10^{13} \text{ m}^2$, so that the radar cross section, at 412.85 Mc/s, represents 0.074 of the projected area. The manner in which the effective cross section of the moon may be proportioned between "gain" and "reflectivity" figures has been the subject of some discussion [2, 7, 8]. If an element of surface is assumed to scatter in a fairly directional manner, for example according to $(\cos \theta)^k$, where typical k values may be 30, 40, 50, etc., then most of the return is given by the central portion of the moon, and the "gain" of the moon as a reflector, relative to its cross sectional area, approaches 4. With this sort of model, which is not critical at all, the power reflectivity must be of the order of 0.02. Values of 0.1 have been quoted, which appear to be high, even allowing for a possible 3-db error in the measurements.

The predictability of the rapid fading rate of a moon-reflected signal is of interest when considering the effects of the ionosphere upon transmission of a UHF signal. The signal is fairly well described when its average amplitude is known, the Faraday rotation allowed for, the Doppler shift computed, and the fading rate predicted to within a constant factor. Changes in the transmission medium, for example, auroral effects, then may be investigated by measuring their effects upon the known characteristics of the undisturbed signal. As mentioned in the introduction, such an experiment has been carried out between Alaska and Massachusetts. This experiment will be described in a forthcoming article.

The authors thank the members of Lincoln Laboratory who contributed to this experiment. They are particularly indebted to S. C. Wang for his discussion of the libration calculations, and to J. C. James for his assistance in reading and correcting the manuscript.

7. References

- [1] C. G. Little, W. M. Thayton, and R. B. Root, Review of ionospheric effects at VHF and UHF, Proc. IRE **44**, 992 (1956).
- [2] I. C. Browne et al., Radio echoes from the moon, Proc. Phys. Soc. B **69**, 901 (1956).
- [3] S. J. Fricker, R. P. Ingalls, W. C. Mason, M. L. Stone, and D. W. Swift, Characteristics of moon-reflected UHF signals, Tech. Rept. 187, Lincoln Lab., M.I.T. (Dec. 1958).
- [4] S. O. Rice, Mathematical Analysis of Random Noise, Bell System Tech. J. **23**, 282 (1944); **24**, 46 (1945).
- [5] J. H. Trexler, Lunar radio echoes, Proc. IRE **46**, 286 (1958).
- [6] B. S. Yapple et al., Radar echoes from the moon at a wavelength of 10 cm, Proc. IRE **46**, 293 (1958).
- [7] J. V. Evans, Research on Moon Echo Phenomena, Tech. Note No. 1 (1 May 1956 to 30 Apr. 1957) Univ. Manchester, England.
- [8] D. D. Grieg, S. Metzger, and R. Waer, Considerations of moon-relay communication, Proc. IRE **36**, 652 (1948).

(Paper 64D5-81)